POLITECNICO DI TORINO
Repository ISTITUZIONALE

5G beamforming implementation and trade-off investigation of cylindrical array arrangements

(Article begins on next page)

30 November 2023

5G beamforming implementation and trade-off investigation of cylindrical array arrangements

Daniel G. Riviello and Francesco Di Stasio

Department of Electronics and Telecommunications (DET)

Politecnico di Torino

Torino, Italy

Email: {daniel.riviello, francesco.distasio}@polito.it

Abstract—**In this paper, we study the performance of a 5G network working at mmW range for the uplink. We consider a single base station scenario equipped with a cylindrical array and a circular array (which can be seen as a single ring cylindrical array), isotropic and directive antenna elements are taken into account and we evaluate the trade-off between antennas per ring and number of rings with fixed number of total antennas. Users are modeled as a spatial Binomial point process in a hexagonal cell. As beamforming techniques, Conventional and Capon algorithms have been considered. As main KPI to evaluate system performance, we consider average achievable per-user rate with different system configurations, such as network loading. The key result of the trade-off investigation is that, when the radius of the cell is much larger than the height of the base station, the best performance occurs when the cylindrical array degenerates in a circular array both when users lay at ground level and with random heights.**

Index Terms—**Beamforming, cylindrical array, circular array, 5G, mmW.**

I. INTRODUCTION

Next generation in wireless communication present extremely challenging issues for researchers and engineers. The increasing data demand over cellular networks requires a hand in hand improvement in achievable channel capacity. In order to meet the new requirements, the use of millimeter-wave frequency spectrum seems to be one of the most promising solutions: hundreds of times more capacity than current 4G cellular networks are expected to be achieved. The great amount of available bandwidth in the related frequency range makes mmW spectrum a strong candidate for deployment in next generation 5G cellular systems [1]. It is well known that in the mmW range the available spectrum is up to 200 time greater than all current cellular allocations [2]–[4].

The use of small wavelengths allows new techniques such as the implementation of massive MIMO antenna systems, array processing and beamforming (BF). Nevertheless, at these frequencies, several communication impairments have to be faced: path loss increase, attenuation due to environmental factors, interference due to mutual coupling in the base station array and so on. All these factors can significantly increase the outage probability. The higher path attenuation can be compensated by the high array gain obtained from the use of large number of antennas. The latter brings more degrees of freedom, so that advanced BF techniques can be implemented in order to manage the inter-user interference. Several

massive MIMO and BF algorithms have been proposed for 5G networks using mainly Uniform Linear Arrays (ULAs) or Uniform Planar Arrays (UPAs) [5]–[7].

In the LTE scenario, the most common base station (BS) equipment considers a trisectorized planar array (120° per sector), which may suffer from beam broadening and pattern degradation as the beam is steered toward azimuths or elevations angles far from broadside. On the other hand, conformal arrays, such as circular or cylindrical ones, have almost isotropic behavior, i.e., the beam can be scanned in discrete steps through an arc while maintaining a constant pattern [8]. Uniform Cylindrical Array (UCylA) can be obtained by stacking circular arrays one above the other and shaping linear arrays over the vertical direction [9], [10]. The circular structure provides 360 degrees symmetry and by stacking in the vertical direction brings increased gain and directivity. In [10] it is shown that a good cylindrical array would require a very large number of antennas, thus making it unfeasible. However, with the advent of mmW communications, placing a very large number of small antennas does not represent anymore a big issue, which makes cylindrical arrays more appealing for future 5G networks.

In this paper, we evaluate the performance of a 5G mmW based network. We consider an uplink scenario for a single BS equipped with a Uniform Cylindrical Array with both isotropic and directive antennas capable of performing directional beamforming. For the latter, we take into account advanced BF techniques, such as conventional and Minimum Variance Distortionless Response (MVDR) or Capon BF [11]. We use some stochastic geometry concepts [12], [13], as single-antenna users are distributed according to a Binomial point process in $\mathcal{R}^2$. We consider the situation with all the users at the same height (ground level), representing an open square scenario. We evaluate the cylindrical behavior in terms of the number of elements on vertical direction and the trade-off between antennas per ring and number of rings with fixed number of total antennas N. The trade-off for array alignment is also evaluated for different cell radius and BS height, with users laying at ground level but also with random heights, i.e., uniformly distributed between ground level and BS height. The results are provided in terms of average per-user achievable rate with different system configuration, such as traffic loading, BF technique and antenna type.

The paper is organized as follows: Sec. II describes the system model, Sec. III illustrates the mathematical framework for circular and cylindrical arrays, in Sec. IV, the beamforming techniques and examples of array radiation patterns with both BF techniques are presented. The results are shown and discussed in Sec. V and finally Sec. VI draws the conclusions.

II. SYSTEM MODEL

Let us consider an hexagonal cell of circumradius R, i.e. the radius of the circumscribed circle or circumcircle, in which K single-antenna users communicate with a Base Station (BS) located at the center of the hexagon, with height h from the ground equipped with an array of N antennas.

A. Spatial point process

Users are modeled as a spatial Binomial point process (BPP) with height equal to zero, i.e. laying at ground level. If we consider a bounded region $\mathcal{A}$ of the plane, with $|\mathcal{A}| = \pi R^2$ the area of the circumcircle, and M the number of nodes existing in the region $\mathcal{A}$, then the number of nodes in the bounded area $\mathcal{B} \subset \mathcal{A}$, with $|\mathcal{B}| = \frac{3\sqrt{3}}{2} R^2$ the area of the hexagon, is a random variable denoted by $\Phi(\mathcal{B})$. The probability of K nodes existing in $\mathcal{A}$ is given by:

$$\Pr[\Phi(\mathcal{B}) = K] = \binom{M}{K} \left(\frac{|\mathcal{B}|}{|\mathcal{A}|}\right)^K \left(1 - \frac{|\mathcal{B}|}{|\mathcal{A}|}\right)^{M-K} \quad (1)$$

i.e., K is a Binomial random variable $Bin(n, p)$ with parameters $n = M$ and probability $p = \frac{|\mathcal{B}|}{|\mathcal{A}|} = \frac{3\sqrt{3}}{2\pi}$:

$$K \sim Bin\left(M, \frac{3\sqrt{3}}{2\pi}\right). \quad (2)$$

1) Users' location: By definition of a BPP, the nodes are conditionally independent and uniformly distributed in the hexagon. Hence, the locations of the randomly deployed K users can be generated in terms of $x - y$-coordinates. Let us denote with X the abscissa of the user in the hexagon, X is the marginal random variable of a uniform 2D distribution in the hexagon. If we consider two random variables X_1 and X_2 where:

$$X_1 \sim \mathcal{U}\left(-\frac{3}{4}R, \frac{3}{4}R\right) \quad (3)$$

$$X_2 \sim \mathcal{U}\left(-\frac{1}{4}R, \frac{1}{4}R\right) \quad (4)$$

then we have

$$X = X_1 + X_2 \quad (5)$$

i.e., X is the sum of two uniform random variables with different bounds, the probability density function (*pdf*) of X is the convolution of the two uniform *pdf*s and it is hence a trapezoidal distribution.

Given the abscissa of a user in the hexagon, the distribution of $Y|X = x$, where Y is the ordinate of the user, is given by

$$\begin{cases} \mathcal{U}\left(-\frac{\sqrt{3}}{2}R, \frac{\sqrt{3}}{2}R\right) & |x| \leq R/2 \\ \mathcal{U}\left(-\sqrt{3}(R - |x|), \sqrt{3}(R - |x|)\right) & |x| > R/2. \end{cases} \quad (6)$$

2) Users' height: Let us denote with Z the height of the user. We consider throughout the paper an open square scenario, in which all users lay at the ground level, hence, $Z = 0$.

In the trade-off analysis for array alignment, we also consider for comparison a dense urban scenario, in which users' heights are uniformly distributed between the ground level and the height of the BS, hence

$$Z \sim \mathcal{U}(0, h) \quad (7)$$

where h denotes the height of the BS.

B. Baseband model

We focus on the uplink communication between K users and the BS . Let $\mathbf{x} = [x_1, x_2, \ldots, x_K]^T$ be the vector of symbols transmitted by the K users in a given time slot and carrier, each with power $E[|x_i|^2] = P_i$. The baseband equivalent signal vector received by the N antennas at the BS is hence given by:

$$\mathbf{y} = \mathbf{H}\mathbf{x} + \mathbf{n} \quad (8)$$

where $\mathbf{H} = [\mathbf{h}_1, \mathbf{h}_2, \ldots, \mathbf{h}_K]$ is the $N \times K$ wireless channel matrix. Each vector $\mathbf{h}_i \in \mathcal{C}^{N \times 1}$ represents the propagation channel vector from user i to the BS and $\mathbf{n} \sim \mathcal{CN}(0, \sigma_n^2 \mathbf{I})$ is the spatially uncorrelated Gaussian noise vector. A simplified channel model, nevertheless suitable for mmW systems, is taken into account. The propagation in mmW bands is mostly Line of Sight (LOS) with a diffusive component [2], The channel vector for the i-th user is

$$\mathbf{h}_i = \sqrt{\gamma_i}\, \beta_i\, \mathbf{a}(\theta_i, \phi_i) \quad (9)$$

where the path loss γ_i is equal to:

$$\gamma_i = \left(\frac{\lambda}{4\pi d_i}\right)^2 \quad (10)$$

with d_i the distance of the i-th user from the BS and β_i is the Rician fading gain affecting the link between the i-th user and the BS with Rician factor R_F:

$$\beta_i \sim \mathcal{CN}\left(\sqrt{\frac{R_F}{R_F + 1}}\, e^{j\xi}, \frac{1}{R_F + 1}\right) \quad (11)$$

with $\xi \sim \mathcal{U}(0, 2\pi)$. In addition, $\mathbf{a}(\theta_i, \phi_i)$ represents the steering vector (SV) or array response for the Direction of Arrival (DoA) of the i-th user with elevation angle θ_i and azimuth ϕ_i. In order to guarantee fairness among users, we adopt a simple power control mechanism and we assume that each user is assigned a transmit power P_i that is a fraction of the maximum transmit power P_{max} and compensates for the path loss:

$$P_i = \frac{d_i^2}{h^2 + R^2}\, P_{max}. \quad (12)$$

We make the following assumptions:

- decoding of the users' signals is performed at the BS with knowledge of channel state information (CSI);
- the BS can obtain long-term averaged over the fading CSI for each user;

- users communicate in the same time slot or resource;
- the BS resorts only to Space Division Multiple Access (SDMA) through BF;
- the BS is able to process all K users' signals, implying no limitation on the number of RF chains, i.e., the BS is able to employ at least K parallel beamformers.

The BS processes the K signals through the combining matrix $\mathbf{B} = [\mathbf{b}_1^H | \mathbf{b}_2^H | \dots | \mathbf{b}_K^H] \in \mathcal{C}^{K \times N}$, where $\mathbf{b}_i$ is the $N \times 1$ beamformer or spatial filter designed for the i-th signal of interest with DoA (θ_i, ϕ_i), so that it attenuates all the other DoAs. The final estimated signal ensemble is given by

$$\hat{\mathbf{x}} = \mathbf{B}\mathbf{y} \tag{13}$$

with decision variable for the i-th user $\hat{x}_i = \mathbf{b}_i^h \mathbf{y}$. We can finally express the instantaneous Signal-to-Noise-plus-Interference ratio at decision variable $\hat{x}_i$ as:

$$SINR_i = \frac{P_i \, |\mathbf{b}_i^H \mathbf{h}_i|^2}{\sigma_n^2 |\mathbf{b}_i|^2 + \sum_{\substack{k=1 \\ k \neq i}}^{K} P_k |\mathbf{b}_i^H \mathbf{h}_k|^2}. \tag{14}$$

The achievable rate for each user i is defined as:

$$C_i = \log_2(1 + SINR_i). \tag{15}$$

Results in this paper will be presented with the metric of the average per-user achievable rate $C = \mathrm{E}[C_i]$ where expectation $\mathrm{E}[\cdot]$ is with respect to fading and users' positions.

III. Array processing

In this Section, we will describe how to express the array response or SV $\mathbf{a}(\theta_i, \phi_i)$ for a generic i-th user when the BS is equipped with a Uniform Circular Array (UCA) or Uniform Cylindrical Array (UCylA) with both isotropic and directive antenna elements. We denote with $N = N_c \cdot N_z$ the total number of available antennas at the BS, where N_c is the number of antennas in each ring, while N_z denotes the number of rings, or equivalently the number of antennas along the z-axis. Perfect calibration of the arrays is assumed with no mutual coupling among the antenna elements.

A. Uniform Circular Array

When the BS is equipped with a single ring of N_c isotropic antennas elements, i.e., a Uniform Circular Array (UCA), we first define the radius of the array as:

$$r = \frac{\lambda N_c}{4\pi} \tag{16}$$

which guarantees $\lambda/2$ spacing on the circular arc between elements. We can then write the $N_c \times 1$ array response or SV $\mathbf{a}_{\text{UCA}}(\theta_i, \phi_i)$ for the DOA of the i-th user as:

$$\mathbf{a}_{\text{UCA}}(\theta_i, \phi_i) = \begin{bmatrix} e^{j\frac{N_c}{2}\sin\theta_i \cos\phi_i} \\ e^{j\frac{N_c}{2}\sin\theta_i \cos\left(\phi_i - \frac{2\pi}{N_c}\right)} \\ \vdots \\ e^{j\frac{N_c}{2}\sin\theta_i \cos\left(\phi_i - 2\pi\frac{N_c-1}{N_c}\right)} \end{bmatrix}. \tag{17}$$

B. Uniform Cylindrical Array

Now we can define a SV for a Uniform Cylindrical Array (UCylA). The array is made of N_z horizontal ring sub-arrays, spaced vertically at half wavelength, with N_c elements per ring. First, we define the $N_z \times 1$ SV of the Uniform Linear Array (ULA) lying on the z-axis as:

$$\mathbf{a}_{\text{ULA}}(\theta_i) = \left[e^{-j\pi\frac{N_z-1}{2}\cos\theta_i}, \dots, e^{j\pi\frac{N_z-1}{2}\cos\theta_i} \right]^T \tag{18}$$

where the phase reference point is the center of the cylinder. The global $N \times 1$ SV of the UCylA is the Kronecker product of the 2 SVs:

$$\mathbf{a}_{\text{UCylA}}(\theta_i, \phi_i) = \mathbf{a}_{\text{UCA}}(\theta_i, \phi_i) \otimes \mathbf{a}_{\text{ULA}}(\theta_i, \phi_i). \tag{19}$$

C. Directive antenna elements

We now redefine the expressions of the SVs when the array is equipped with directive antenna elements. Directivity is assumed only for the azimuthal plane, while the antennas are isotropic w.r.t. the elevation angle, therefore we define the directivity function of the single antenna as:

$$D(\phi_i) = \begin{cases} u\cos(\phi_i - \delta) & \text{for } -90° + \delta < \phi_i < 90° + \delta \\ 0 & \text{otherwise} \end{cases} \tag{20}$$

where u is a scaling factor and δ the azimuthal direction to which the antenna element is pointed.

1) Circular array with directive elements: Let us denote with $\mathbf{d}(\phi_i)$ the $N_c \times 1$ vector, which contains the values of the directivity function $D(\phi_i)$ associated with each element of the UCA:

$$\mathbf{d}(\phi_i) = \begin{bmatrix} u\cos\phi_i \\ u\cos\left(\phi_i - \frac{2\pi}{N_c}\right) \\ \vdots \\ u\cos\left(\phi_i - 2\pi\frac{N_c-1}{N_c}\right) \end{bmatrix}. \tag{21}$$

It is easy to verify that, due to shadowing, half of the elements will be equal to zero in accordance with (20). The resulting $N_c \times 1$ SV of the UCA with directive antenna elements is equal to:

$$\mathbf{a}_{\text{UCA}}^{(d)}(\theta_i, \phi_i) = \mathbf{d}(\phi_i) \odot \mathbf{a}_{\text{UCA}}(\theta_i, \phi_i) \tag{22}$$

where $\odot$ denotes the Hadamard (entrywise) product.

2) Cylindrical array with directive elements: The $N \times 1$ SV for a UCylA with directive antenna elements becomes:

$$\mathbf{a}_{\text{UCylA}}^{(d)}(\theta_i, \phi_i) = \mathbf{a}_{\text{UCA}}^{(d)}(\theta_i, \phi_i) \otimes \mathbf{a}_{\text{ULA}}(\theta_i, \phi_i). \tag{23}$$

IV. Beamforming methods

We focus now on the design of the beamformer $\mathbf{b}_i$ design whose tasks are to correctly estimate the i-th signal of interest and attenuate interferers. Two different algorithms are taken into account for analysis:

1) Conventional BF,
2) Minimum Variance Distortionless Response (MVDR) BF or Capon BF.

A. Conventional beamforming

With this approach, also known as beam steering, the BS produces a phase shift to compensate for the delay of the DOA (θ_i, ϕ_i) for the i-th user, which is given by:

$$\mathbf{b}_i = \mathbf{a}(\theta_i, \phi_i). \tag{24}$$

B. MVDR beamforming

For MVDR BF, we first introduce the global spatial covariance matrix of noise plus interference for:

$$\mathbf{R} = \sigma_n^2 \mathbf{I} + \sum_{k=1}^{K} P_k \, \gamma_k \, \mathbf{a}(\theta_k, \phi_k) \, \mathbf{a}^H(\theta_k, \phi_k). \tag{25}$$

Beamforming is then a constrained optimization problem that maximizes the power towards the i-th user of interest and minimizes the overall interference arising from other DoAs [11]:

$$\mathbf{b}_i = \frac{\mathbf{R}^{-1} \, \mathbf{a}(\theta_i, \phi_i)}{\mathbf{a}^H(\theta_i, \phi_i) \, \mathbf{R}^{-1} \, \mathbf{a}(\theta_i, \phi_i)}. \tag{26}$$

Notice that the denominator $\mathbf{a}^H(\theta_i, \phi_i) \, \mathbf{R}^{-1} \, \mathbf{a}(\theta_i, \phi_i)$ in (26) is a normalization factor and ensures unitary gain at the DoA of interest.

C. Patterns with isotropic and directive antennas

The array gain function, when the beamformer is designed for the DoA (θ_i, ϕ_i) of the i-th user, can be defined for any DoA (θ, ϕ) as $\mathbf{G}(\theta, \phi \,|\, \theta_i, \phi_i) = |\mathbf{b}_i \, \mathbf{a}(\theta, \phi)|^2$, the array radiation pattern or array factor AF is equal to $AF(\theta, \phi \,|\, \theta_i, \phi_i) = \sqrt{\mathbf{G}(\theta, \phi \,|\, \theta_i, \phi_i)}$ and in the case conventional BF it has very well known expressions for linear, planar [14], [15] and circular arrays [8].

By defining $G_{max} = \max_\theta \mathbf{G}(\theta, \phi \,|\, \theta_i, \phi_i)$, it is known that for a conventional beamformer with isotropic elements $G_{max} = N$ [8], [15]. For a UCylA with directive elements, G_{max} can be defined as:

$$G_{max} = N_z \sum_{n=N_c/4}^{N_c/4} u^2 \cos\left(\frac{2\pi n}{N_c}\right) \tag{27}$$

for large N_c, the summation can be approximated with the integral:

$$G_{max} \approx N_z \, u^2 \frac{N_c}{2\pi} \int_{-\pi/2}^{\pi/2} \cos^2(\phi) \, \mathrm{d}\phi = N_z \, u^2 \frac{N_c}{2\pi} \frac{\pi}{2} = u^2 \frac{N}{4}. \tag{28}$$

Finally, by choosing $u = 2$, we ensure $G_{max} = N$ for both array configurations. Fig. 1 shows the radiation pattern with conventional BF for a DoA $(100°, 45°)$ of a UCylA with 4 rings along z and 36 isotropic (directive) elements per ring on the top (bottom). By focusing on the azimuthal plane, the beam remains constant for the UCA regardless of ϕ and the main lobe is wider with directive antennas w.r.t. isotropic ones, since half of the elements actually contribute to the pattern, but it is worth noticing that for the same reason, sidelobes are almost suppressed, and thus directive elements
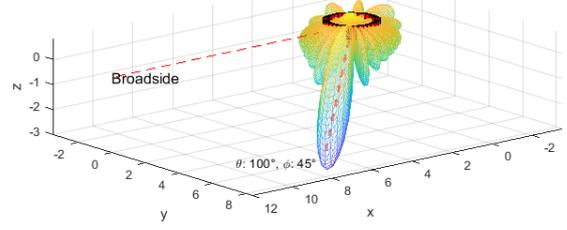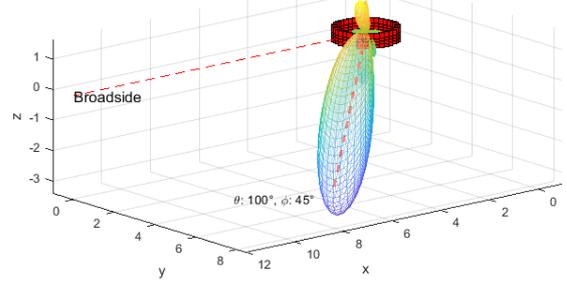

Fig. 1: Pattern with conventional BF for a 36×4 UCylA for DoA $(100°, 45°)$ with isotropic and directive antenna elements.

can significantly improve the interference rejection capability in conventional beamforming.

Fig. 2 shows an example of pattern with MVDR BF with isotropic (on the left) and directive (on the right) antenna elements with the same configuration of Fig. 1, the user of interest has DoA $(90°, 0°)$, while the 5 interferers have DoAs: $(90°, -10°)$, $(98°, -15°)$, $(92°, 10°)$, $(94°, 20°)$ and $(100°, 30°)$. It can be noticed how MVDR BF techniques tries to minimize the gain for the aforementioned DoAs.

V. RESULTS

We compare now the performance of a BS equipped with a UCylA with both isotropic and directive antennas in terms of average-per-user rate with both conventional and MVDR BF. First, we summarize all simulation parameters in Tab. I

Fig. 3 shows the average per-user rate C as a function of the network load or average number of users in the hexagonal cell $\mathcal{B}$, computed as the mean of a Binomial random variable $\mathrm{E}(K) = M \frac{3\sqrt{3}}{2\pi}$, with M ranging from 20 to 200 users in the circumcircle, the UCylA has $N = 180$ total antennas, with $N_c = 45$ rings and $N_z = 4$ elements per ring. It clearly confirms how MVDR is able to outperform conventional BF thanks to its improved interference rejection capability, but it also shows that directive elements provide a significant rate improvement w.r.t. isotropic elements for conventional BF. The gap is more than 2 bps/Hz for low network loads and
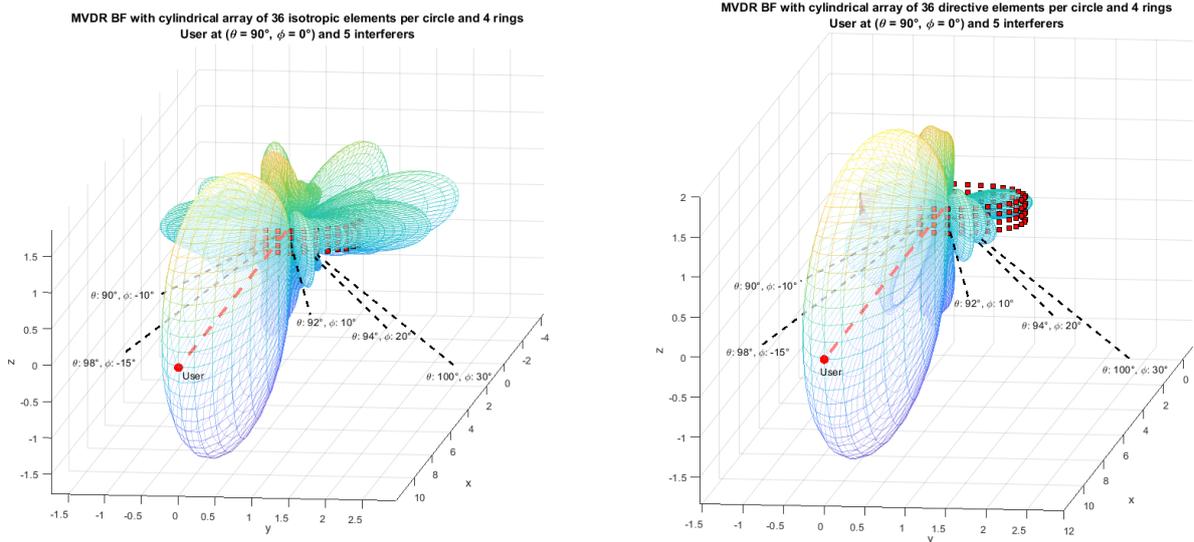
Fig. 2: Pattern with MVDR BF for a 36×4 UCylA for DoA $(90°, 60°)$ with isotropic and directive antenna elements.

Parameter	Value
Carrier frequency f_c	28 GHz
Bandwidth B	100 MHz
Height of the BS h	15 m
Noise figure F	7 dBm
Maximum TX power P_{max}	20 dBm
Total antennas N	180
Directivity function $D(\phi_i)$	$2\cos(\phi_i - \delta)$
Circumradius of the cell R	100 m
Network load (number of users M in $\mathcal{A}$)	60
Rician factor R_F	10

TABLE I: Simulation parameters.

Fig. 3: Average per-user rate as a function of the network load (average number of users in $\mathcal{B}$). Comparison for a UCylA with isotropic and directive antennas, implementing conventional and MVDR BF, $N_c = 45$, $N_z = 4$, $R = 100$ m, $h = 15$ m.

it reduces as the network load increases as well as the overall performance; for the MVDR BF case, the overall performance decreases more slowly and the gap between directive and isotropic antennas is much smaller, but it slightly increases as the number of users increases.

Now, we investigate on the distribution of antenna elements along the vertical axis and the azimuthal plane by keeping constant the total number of antennas N. Fig. 4 shows the average per-user rate with a cell circumradius $R = 100$ m and BS height $h = 15$ m for different configurations of N_c antennas per ring and N_z rings or antennas along the z-axis, with fixed $N = 180$, both isotropic and directive elements with conventional (above) and MVDR (below) BF, $M = 60$ users in the area $\mathcal{A}$ both at ground level and with random heights. It can be noticed that both when users lie on a plane at the ground level ($h = 0$) or they have random height, the best performance occurs when all antennas are arranged in a single UCA or ring: this suggests that producing narrower
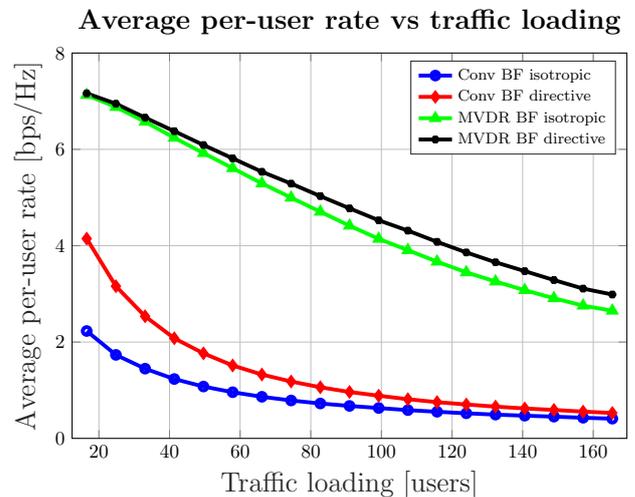
beams along ϕ offers better interference rejection capability than along θ when $R \gg h$. It can also be noted that in the configuration $N_z = 180$, $N_c = 1$, the array degenerates into a ULA along z (only isotropic elements are used for this specific configuration). Finally, Fig. 5 shows the average rate for the same configurations of Fig. 4, but with a cell circumradius $R = 75$ m and BS height $h = 35$ m, here the gap between users with random heights and the ones laying at the ground is clearly visible, and it increases as the array increases the number of rings (especially for MVDR BF). The vertical ULA with $N_z = 180$ becomes also very competitive for conventional BF.
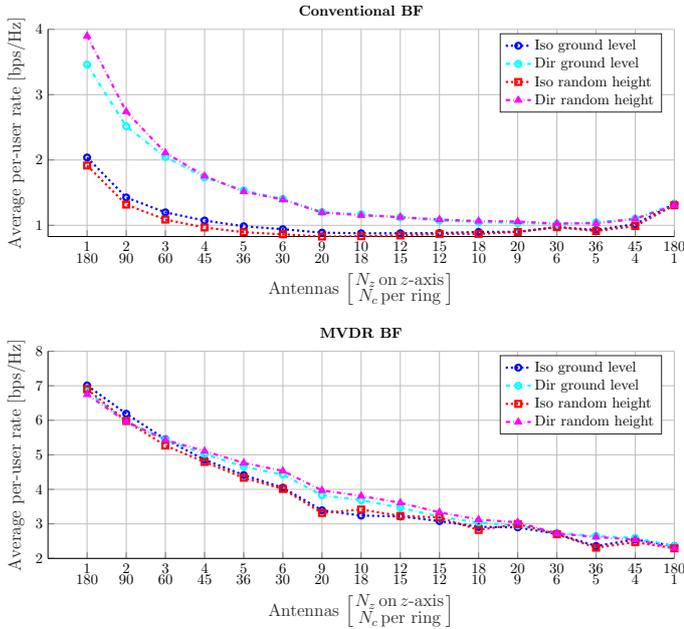
Fig. 4: Average per-user rate in UCylA for different number of rings N_c and antennas along z-axis N_z with both isotropic and directive elements implementing conventional (above) and MVDR (below) BF with $N = N_c \cdot N_z = 180$. Circumradius $R = 100$ m, BS height $h = 15$ m. For $N_c = 1$, $N_z = 180$, antennas are only isotropic. $M = 60$ users.
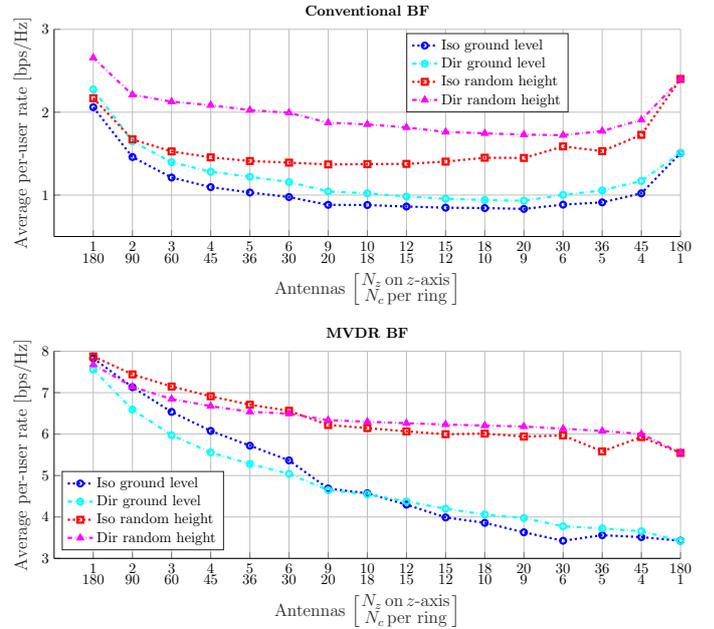

Fig. 5: Average per-user rate in UCylA for different number of rings N_c and antennas along z-axis N_z with both isotropic and directive elements implementing conventional (above) and MVDR (below) BF with $N = N_c \cdot N_z = 180$. Circumradius $R = 75$ m, BS height $h = 35$ m. For $N_c = 1$, $N_z = 180$, antennas are only isotropic. $M = 60$ users.

VI. CONCLUSIONS

The performance of a 5G Base Station equipped with a Uniform Cylindrical Array and working in the mmW region with both isotropic and directive antenna elements has been evaluated. Conventional and Capon beamforming have been considered. The results, shown in the form of achievable average per-user rate with different configurations, have confirmed the improved interference rejection capability of the MVDR technique. The trade-off between antennas per ring and number of rings with fixed number of total antennas has been carried out and it has shown that in the presented scenario, with randomly deployed users in a hexagonal plane (at ground level or random height), the best performance occurs when the cylindrical array degenerates in a circular array for a cell radius much larger than BS height.

REFERENCES

[1] W. Roh, J. Seol, J. Park, B. Lee, J. Lee, Y. Kim, J. Cho, K. Cheun, and F. Aryanfar, "Millimeter-wave beamforming as an enabling technology for 5G cellular communications: theoretical feasibility and prototype results," *IEEE Communications Mag.*, pp. 106-113, Feb. 2014.

[2] M. R. Akdeniz, Y. Liu, M. K. Samimi, S. Sun, S. Rangan, T. S. Rappaport, and E. Erkip, "Millimeter Wave Channel Modeling and Cellular Capacity Evaluation", *IEEE Journal on Selected Areas in Communications*, vol. 32, no. 6, pp. 1164-1179, June 2014.

[3] T. S. Rappaport, W. Roh, and K. Cheun, "Mobiles millimeter-wave makeover," *IEEE Spectrum*, pp. 35-56, Sep. 2014.

[4] S. Han, C. Lin, Z. Xu, and C. Rowell, "Large-scale antenna systems with hybrid analog and digital beamforming for millimeter wave 5G," *IEEE Communications Mag.*, pp. 186-194, Jan. 2015.

[5] R. W. Heath, N. Gonzlez-Prelcic, S. Rangan, W. Roh, and A. M. Sayeed, "An Overview of Signal Processing Techniques for Millimeter Wave MIMO Systems," in *IEEE Journal of Selected Topics in Signal Processing*, vol. 10, no. 3, pp. 436-453, Apr. 2016.

[6] O. E. Ayach, S. Rajagopal, S. Abu-Surra, Z. Pi, and R. W. Heath, "Spatially Sparse Precoding in Millimeter Wave MIMO Systems," in *IEEE Transactions on Wireless Communications*, vol. 13, no. 3, pp. 1499-1513, Mar. 2014.

[7] A. Alkhateeb, J. Mo, N. Gonzalez-Prelcic, and R. W. Heath, "MIMO Precoding and Combining Solutions for Millimeter-Wave Systems," in *IEEE Communications Magazine*, vol. 52, no. 12, pp. 122-131, Dec. 2014.

[8] L. Josefsson and P. Persson, *Conformal Array Antenna Theory and Design*, John Wiley, Hoboken, NJ, Chapter 6, 2006.

[9] E. Yaacoub, M. Husseini, and H. Ghaziri, "An overview of research topics and challenges for 5G massive MIMO antennas", *2016 IEEE Middle East Conference on Antennas and Propagation (MECAP)*, pp. 1-4, Sep. 2016.

[10] E. Yaacoub, K. Y. Kabalan, A. El-Hajj, and A. Chehab, "Cylindrical antenna arrays for WCDMA downlink capacity enhancement", in *2006 IEEE International Conference on Communications*, vol. 11, pp. 4912-4917, Jun. 2006.

[11] J. Capon, "High-Resolution Frequency-Wavenumber Spectrum Analysis," *Proceedings of the IEEE*, vol. 57, no. 8, pp. 1408-1418, Aug. 1969.

[12] M. Haenggi, "On distances in uniformly random networks", *IEEE Transactions on Information Theory*, vol. 51, no. 10, pp. 3584-3586, Oct. 2005.

[13] S. Srinivasa and M. Haenggi, "Distance Distributions in Finite Uniformly Random Networks: Theory and Applications", *IEEE Transactions on Vehicular Technology*, vol. 59, no. 2, pp. 940-949, Feb. 2010.

[14] Constantine A. Balanis, *Antenna theory: analysis and design*, Wiley-Interscience, 2005.

[15] Harry L. Van Trees, *Optimum Array Processing: Part IV of Detection, Estimation, and Modulation Theory*, John Wiley & Sons, 2004.